Journal of Alloys and Compounds 599 (2014) 121–126

Contents lists available at ScienceDirect

Journal of Alloys and Compounds

journal homepage: www.elsevier.com/locate/jalcom

Phase equilibria in the $ZnGeAs_2$–$CdGeAs_2$ system

Irina V. Fedorchenko [a,c,*], Alexey N. Aronov [a], Lukasz Kilanski [b], Victor Domukhovski [b], Anna Reszka [b], Bogdan J. Kowalski [b], Erkki Lähderanta [c], Witold Dobrowolski [b], Alexander D. Izotov [a], Sergey F. Marenkin [a]

[a] Kurnakov Institute of General and Inorganic Chemistry Russian Academy of Sciences, Leninskiy pr. 31, 119991, Moscow, Russian Federation
[b] Institute of Physics, Polish Academy of Sciences, al. Lotnikow 32/46, 02-668 Warsaw, Poland
[c] Lappeenranta University of Technology, P.O. Box 20, FI-53851 Lappeenranta, Finland

ARTICLE INFO

Article history:
Received 15 December 2013
Received in revised form 14 February 2014
Accepted 15 February 2014
Available online 22 February 2014

Keywords:
Semiconductors
Phase diagrams
SEM
X-ray diffraction
Non-linear optical crystal

ABSTRACT

The phase equilibria in the $ZnGeAs_2$–$CdGeAs_2$ system were investigated by X-ray, DTA, EDXRF, microstructure observations and SEM. The solid solutions are present in all range of concentrations above 440 °C. Below this temperature a decay region of solid solution of $Zn_{1-x}Cd_xGeAs_2$ is observed in the range of concentrations x = 0.19–0.92 at room temperature. The investigation of the system was obstructed by liquation and segregation processes occurring during the synthesis.

1. Introduction

Modern industry of electronics devices gives new tasks to material science and force to look for new materials which explained the interest to the multicomponent semiconductors. During last several years, many reports were published about threefold semiconductors based on $A^{II}B^{IV}C_2^V$ chalcopyrites. These materials are applicable for photovoltaic [1–4], non-linear infrared technique [5–9], laser optics [10–12], spintronics [13–16] applications and others. In earlier reports we showed that chalcopyrites $A^{II}B^{IV}C_2^V$ (where A-Zn, Cd; B-Si, Ge; C-As, P) are perspective for creating the nano- structural ferromagnetic compositions based on them [16,17]. Such compositions are advanced for spintronics applications. These threefold compounds are semiconductors with wide range of energy gap from 0.2 eV to 2.05 eV and crystal structure cognate to doubled sphalerite lattice [17].

In this report we focused on phase equilibria of $ZnGeAs_2$–$CdGeAs_2$ system. In the context of our previous works, $ZnGeAs_2$ and $CdGeAs_2$ were chosen as most investigated and most promising compounds for creating solid solutions. The lattice parameter difference between these compounds is less than 5%, they are isostructural and have close atomic radii of second group elements. The band gap of $ZnGeAs_2$ and $CdGeAs_2$ is 1.15 and 0.57 eV, respectively [18], that is around mostly used IV group semiconductors. Our previous reports showed that magnetogranular structures based on these chalcopyrites have giant magnetoresistance effect [19,20]. The influence of the substitution of zinc atoms by cadmium in the $ZnGeAs_2$ was calculated in theoretical work [21] using WIEN2 k implementation of full potential linearized augmented plane wave (FPLAPW) method. No significant difference in magnitude of total density of state is observed in the vicinity of E_F (Fermi energy) by this substitution. It gives us hope to observe continuous range of substitution solid solutions with smooth changes of lattice parameters and band gap, to manage the structural, electrical and magnetic properties. The successful preparation of the compounds requires optimal technological parameters for each composition of the $Zn_{1-x}Cd_xGeAs_2$ solid solutions. This encourages the interest to investigate phase equilibria into $ZnGeAs_2$–$CdGeAs_2$ system. The phase diagram will used for the growth of novel single crystals for application in non-linear optics and as a host base for nanogranular semiconductor-ferromagnetic structures.

2. Materials and methods

The synthesis of $Zn_{1-x}Cd_xGeAs_2$ solid solutions was made in three steps. First, $ZnAs_2$ and $CdAs_2$ were synthesized by direct interaction of high purity arsenic (99,999%) and zinc and cadmium (99,99%) single crystals, respectively. The syntheses were made in evacuated ($<10^{-6}$ Torr) and sealed ampoules. The resistance furnace with wide non-gradient zone (<0.1°) was used to avoid the volatilization of

* Corresponding author at: Kurnakov Institute of General and Inorganic Chemistry Russian Academy of Sciences, Leninskiy pr. 31, 119991, Moscow, Russian Federation. Tel.: +7 9039735913.
E-mail addresses: fedorkin-san@rambler.ru, fedorchenkoiv@yahoo.com (I.V. Fedorchenko).

http://dx.doi.org/10.1016/j.jallcom.2014.02.085
0925-8388/

Table 1
EXDRF data.

Normalized molar fractions					
N Samples	Zn	Cd	Ge	As	Average Zn/Cd
1	1	0	1	2	–
2	0.82367	0.17633	1	2	0.80597/0.19403
	0.78327	0.21673	1	2	
	0.81042	0.18958	1	2	
3	0.85452	0.14548	1	2	0.84495/0.15505
	0.83510	0.16491	1	2	
4	0.81852	0.18148	1	2	0.76165/0,23835
	0.81335	0.18665	1	2	
	0.65309	0.34691	1	2	
5	0.77449	0.22551	1	2	0.63456/0.36544
	0.49295	0.50705	1	2	
6	0.66116	0.33884	1	2	0.63916/0.36084
	0.61807	0.38193	1	2	
	0.63805	0.36195	1	2	
7	0.43372	0.56628	1	2	0.37989/0.62011
	0.32318	0.67682	1	2	
	0.38315	0.61685	1	2	
8	0.30564	0.69436	1	2	0.32582/0.67418
	0.32645	0.67355	1	2	
	0.34469	0.65531	1	2	
9	0.35743	0.64257	1	2	0.28535/0.71465
	0.27194	0.78806	1	2	
10	0.08951	0.91049	1	2	0.09148/0.90852
	0.08761	0.91239	1	2	
	0.09732	0.90268	1	2	
11	0	1	1	2	–

arsenic to the cool part of the ampoule, as the saturated pressure of arsenic at the temperature of synthesis is quite high. The extra weight of arsenic was calculated by Clapeyron – Clausius equation to compensate the saturated pressure of vapor into the empty volume of the ampoule. The temperature regimes of the synthesis corresponds to the methods described in Ref. [22]. The fabricated crystals were identified using X-ray and microstructure analyses. The precursors were single phase zinc diarsenic and cadmium diarsenic compounds. On the second step the threefold compounds $ZnGeAs_2$ and $CdGeAs_2$ were synthesized by interaction germanium with $ZnAs_2$ and $CdAs_2$, respectively, as described in work [23]. This method of synthesis is chosen to decrease the saturated vapor pressure of arsenic, as it is lower in the double compounds than in pure arsenic. The fabricated samples also were checked with X-ray and microstructures, only single phase crystals were used for preparing $Zn_{1-x}Cd_xGeAs_2$ ($x = 0, 0.1, 0.2...1$) samples. Eleven samples were prepared by mixing the stoichiometric ratios of the compounds and separated by two groups for the synthesis. First group of samples ($x = 0–0.6$) was heated up to 1163 K. Second group of samples ($x = 0.7–1$) was heated up to 1063 K. The separation of the samples was done to avoid the overheating the $CdGeAs_2$-rich compositions. The arsenic pressure in $CdGeAs_2$ is enough high to be a reason of stoichiometric deviation in the compound. The weight of each sample was about 10 g. The samples were heat-treated in the above-mentioned temperature for 2 days. After 24 h for homogenization of the solution melt the furnace was switched off. The samples were cooled down to room temperature during 24 h. All samples were fused. The investigations of the samples were done by X-ray, differential thermal analysis (DTA), microstructures, energy dispersive X-ray fluorescence (EDXRF), and scanning electron microscopy (SEM).

3. Results and discussion

The microstructure analysis was done with optical Epiquant microscope, under one hundredfold magnification. The samples with $x = 0$; 0.1; 0.9 and 1 were single phase, but in the other

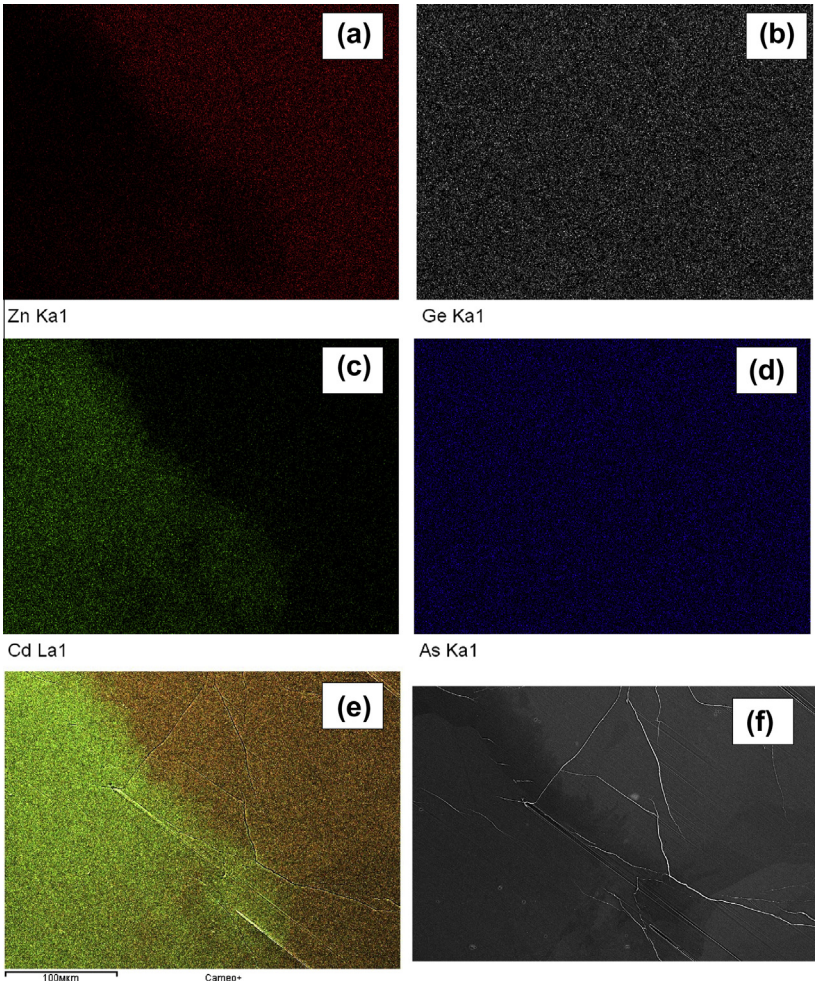

Fig. 1. Distribution of the elements of the sample of solid solution: (a) zinc; (b) germanium; (c) cadmium; (d) arsenic; (e) zinc and cadmium; (f) imagine of the surface.

samples we observed to be two phases. The differential thermal analysis was done on derivatograph ЛВ-2. The accuracy of the data is ±10°. To support these data the samples were studied with EDXRF, X-ray and SEM.

The EDXRF analyses were done with Tracor X-ray Spectrace 5000 Spectrometer equipped with Si(Li) detector. Circular (1.5–2 mm thickness) discs cut from the middle of the samples were used for the measurements. The EDXRF spectra obtained for each individual sample were fitted to the theoretical model assuming the presence of fluorescence Ka lines of Zn, Cd, Ge and As atoms. No other atoms than the ones mentioned above were observed in the EDXRF spectra. It indicated that (if they were present) the concentration of unintentional dopants was lower than 10^{15} cm^{-3}. The relative maximum uncertainty of this method with respect to the calculation of molar fractions of the elements does not exceed 10%. The EDXRF results are gathered in Table 1. The dispersion of the data suggests that the liquation process is present in the samples. It encourages us to make more careful investigations.

The Scanning electron microscope (SEM) investigations were made by two different apparatus. First, Carl Zeiss NVision40 three-beam workstation, equipped with Oxford Instruments X-Max analyzer, at the Center for collective use of physical methods of study Inorganic Chemistry, RAS. The range of accelerating voltages was up 1–20 kV. X-ray microanalysis was performed in scanning mode and a full line of mapping. Fig. 1 shows that distribution of the components is homogeneous except for Zn and Cd. In Fig. 1f it is clearly visible that samples consist of three different areas, two light compounds separated with dark one. Fig. 1e shows that dark area consists both type of zinc and cadmium atoms. Table 2 presents the concentrations along the marked lines in Fig. 2. It is clearly visible that the dark area satisfied uninterrupted compound of solid solutions and at the same time, more bright areas have a sharp border with it, with concentration from 16 till 19 at.% from both sides. These data show some difference with early work. The authors [24] defined the borders of the compounds as not more than 10 wt.% from both sides, these are $Zn_{0.16}Cd_{0.84}GeAs_2$ and $Zn_{0.94}Cd_{0.06}GeAs_2$ respectively. This demands more careful study, as the observed cadmium solubility is bigger than three times from our SEM observation.

A more detailed investigation of the dark area were made by the field emission scanning electron microscopy with the use of Hitachi SU-70 Analytical UHR FE-SEM equipped with the Thermo Fisher NSS 312 energy dispersive X-ray spectrometer system (EDS) equipped with SDD-type detector in the Institute of Physics PAS. The imagine of the dark area is presented in Fig. 3. In Fig. 3a it is clearly visible, that dark area consists of the mixture of the small dispersion granules of solid solutions with both sides. More dark color of this zone is explained by the borders between grains. In Fig 3b and c we show the SEM image at which the small grains are included into the homogeneous material. The formation of these grains is explained by dissipation of the solid solution at the solid state. They were segregated from the saturated solutions with decreasing temperature. The process of segregation goes along the binodal dissipation curve, that is the reason of the different size of the granules. Moreover, as it is visible from Fig. 3c, the distribution of the inclusions is random and the SEM data cannot be correct, as the underlying inclusions will make influence on the SEM data. The same effect is described in the literatures [25–27]. The report [25] described the formation of nanometer-sized (≈70 nm) grains in equimolar ZrC–NbC solid solutions. The authors reported, that the nanostructure remains stable during long-term (100–700 h) annealing between 670 and 1270 K. This way, SEM data requires support the solubility of A^{II} cations.

The powder X-ray diffraction method was used to correct the solubility data. The diffraction patterns were obtained with Cu-radiation ((Cu K_{a1}) = 1.54056 Å) with the use of the Siemens D-5000 diffractometer (E = 40 keV, I = 25 mA, t = 8 s/point, step = 0.02°). The calculations of lattice parameters and existing phases were made by TRIOR program, Table 3. All samples from x = 0.1–0.9 had two phases, namely $ZnGeAs_2$ and $CdGeAs_2$. The lattice parameters for single phase samples NN 1 and 11 are in good agreement with literature data (ICDD). The solid solutions with chemical content near both $ZnGeAs_2$ and $CdGeAs_2$ alloy have changes of the lattice parameters depending from the concentration of the opposite component. As the chosen compounds have the same crystal structure, close values of the lattice parameters, difference of atomic radii is less than 12% and approximate valence shell of the atom and the difference of the electronegativity is 0.04 (Pauling scale), it is logical to suppose that these compounds will form substitutional solid solutions which have to obey the Vegard's law. Vegard law for the "a" parameter can be written as:

$$a_{Zn_{1-x}Cd_xGeAs_2} = a_{ZnGeAs_2} \cdot x + (1-x)a_{CdGeAs_2} \quad (1)$$

On the other hand, the calculation of the cell parameters was made through X-ray patterns present in Table 3. Comparing these data, the conclusions about solubility of the components can be correct. In Fig. 4 the hypothetical Vegard's law line for $ZnGeAs_2$–$CdGeAs_2$ solid solutions and the biggest changes of the lattice parameter calculated with X-ray data are presented. The crossing of these lines determines the maximum solubility of the components (can be calculated from Eq. (1). According to Fig. 4 the border compounds have compositions $Zn_{0,08}Cd_{0,92}GeAs_2$ and $Zn_{0,81}Cd_{0,19}GeAs_2$. These data are different from early work [24].

The results of the EDXRF, microstructures, X-ray and DTA are listed in Table 4. The recalculation of the X-ray data to the concentration of zinc and cadmium ions were done taking in account the phase relations and concentration of the component in solid solutions determined by the Vegard law. The presence of the cubic structure in the solid solutions was reported in the literature [28]. The difference of the data of the composition of the samples can be explained by the nanosized (20–40 nm) inclusions into

Table 2
SEM data of surface in Fig. 2.

Specter	Zn (at.%)	Cd (at.%)	Ge (at.%)	As (at.%)
1	4.0	21.4	23.6	51.1
2	4.4	20.6	23.8	51.2
3	4.6	20.6	23.9	50.9
4	4.5	20.1	24.2	51.1
5	5.0	19.8	24.0	51.2
6	6.7	18.3	23.7	51.3
7	7.4	17.7	24.1	50.8
8	8.1	17.7	23.0	51.2
9	9.8	15.2	24.0	51.0
10	11.3	13.1	23.8	51.7
11	15.1	9.2	23.6	52.1
12	11.0	13.9	23.8	51.2
13	7.8	17.5	23.2	51.4
14	8.1	16.9	23.7	51.2
15	10.0	15.5	23.3	51.1
16	9.4	16.1	24.4	50.1
17	9.0	16.9	23.7	50.7
18	9.7	16.1	23.6	50.5
19	11.4	14.0	24.2	50.4
20	12.4	13.9	23.8	49.9
21	19.9	5.4	23.8	50.9
22	5.1	20.0	24.0	51.0
23	4.9	20.3	24.3	50.5
24	6.2	18.9	23.7	51.3
25	7.6	17.7	23.5	51.2
26	10.1	15.4	22.7	51.8
27	13.5	12.7	21.0	52.9
28	20.4	5.1	22.8	51.7
29	21.2	4.2	23.1	51.5

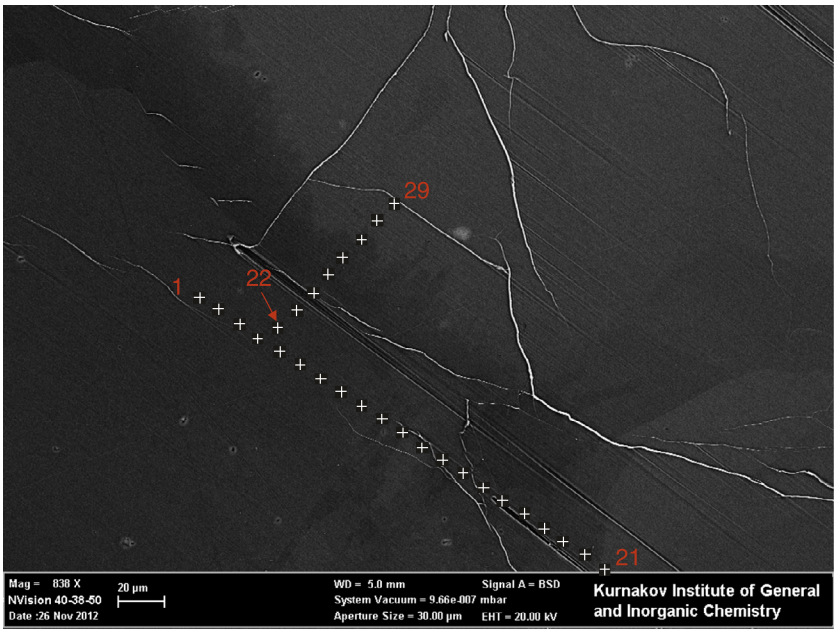

Fig. 2. SEM imagine of the solid solution.

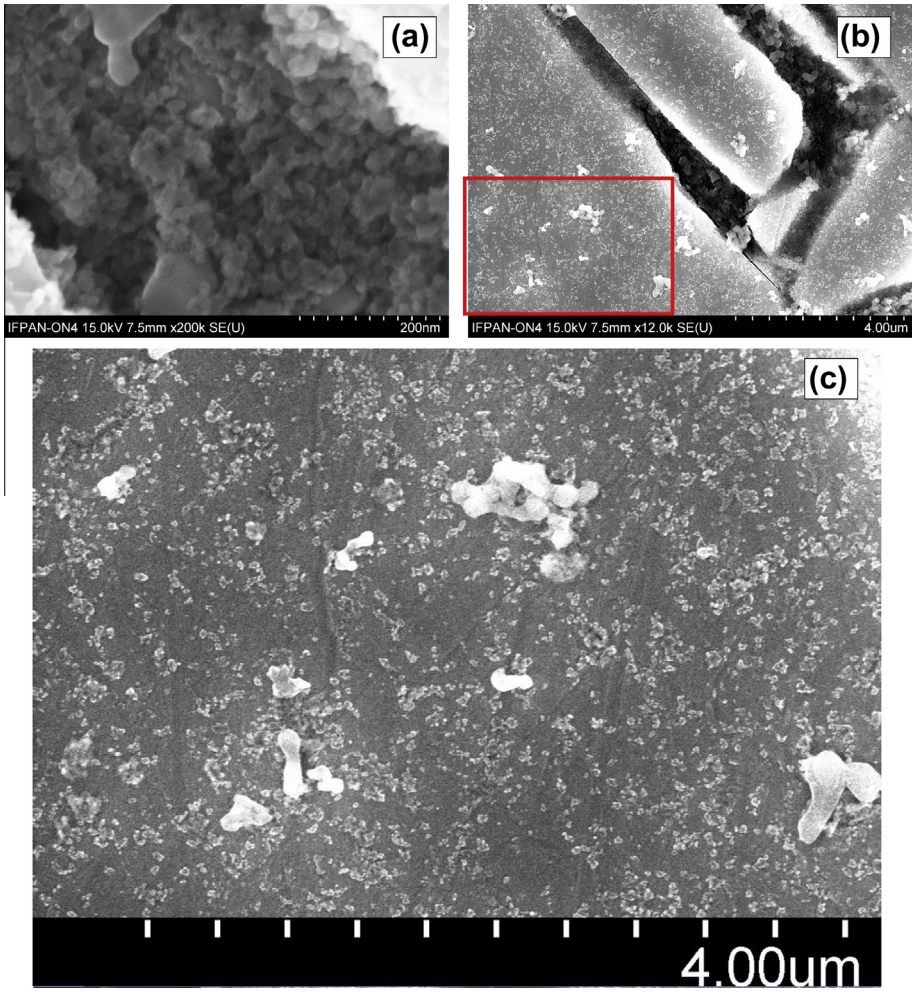

Fig. 3. SEM imagine of the solid solution (a) the mix of the granules of the border compounds; (b) solid solution and mix of the granules; (c) solid solution with segregated granules.

Table 3
X-ray data of solid solutions $Zn_xCd_{1-x}GeAs_2$ (x = 0, 0.1, 0.2…1).

NN	Compounds from $ZnGeAs_2$ side (Phase A)	$a = b$, A [ICDD]	Compounds from $CdGeAs_2$ side (Phase B)	$a = b$, A [ICDD]	Phase relation, mol.% A/B
	$ZnGeAs_2$	5.6700 [04-008-2039]	$CdGeAs_2$	5.9410 [04-012-7941]	
	$ZnGeAs_2$	5.6720 [36-1328]	$CdGeAs_2$	5.9440 [04-012-7942]	
	$ZnGeAs_2$	5.6720 [04-001-5357]			
1	$Zn_{1-x}Cd_xGeAs_2$	5.67162	$Zn_{1-x}Cd_xGeAs_2$	–	100.0/0.0
2		5.67168		5.92073	94.5/5.5
3		5.67352		5.92158	86.6/13.4
4		5.67369		5.92118	72.9/27.1
5		5.67336		5.91876	71.4/28.6
6		5.67890		5.92933	60.8/39.2
7		5.68175		5.92653	47.0/53.0
8		5.70387		5.92891	38.1/61.9
9		5.71639		5.93082	19.1/80.9
10		5.72285		5.93213	2.6/97.4
11		–		5.94184	0.0/100.0

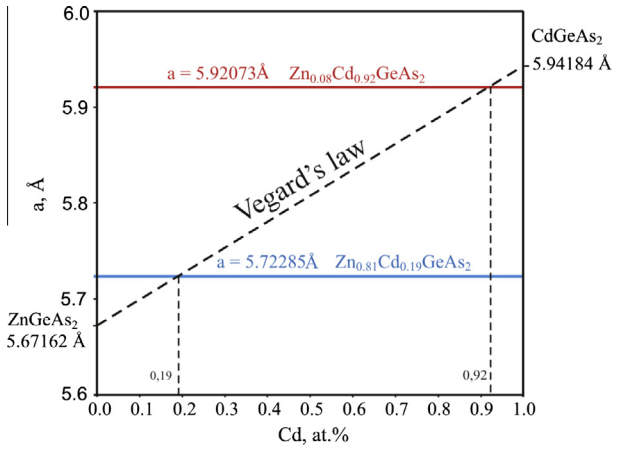

Fig. 4. Vegard's law and lattice parameters of solid solutions.

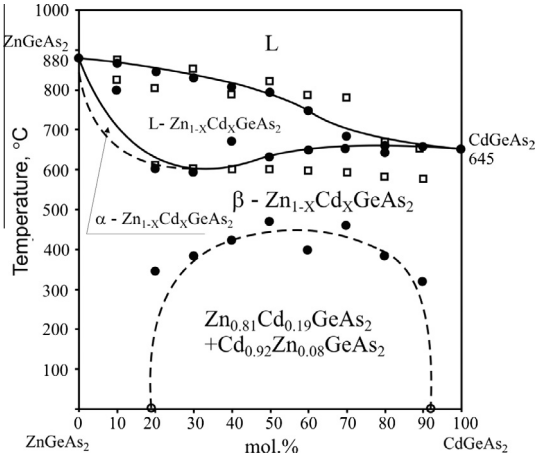

Fig. 5. Phase diagram $ZnGeAs_2$–$CdGeAs_2$.

the solid solutions with different concentration (Fig. 3(c)). These inclusions form when cooling the samples. They are stable, as the dissipation of the solid solution happen at the low temperature (440 ± 10 °C) and lower (along the binodal dissipation), and therefore practically no diffusion occurs in solid state into the crystal. It should be mentioned that no other phases were observed by the X-ray diffraction. At the same time, EDXRF data match the stoichiometric proportions of solid solutions $Zn_{1-x}Cd_xGeAs_2$. So, there are no doubts that segregated inclusions are compounds of solid solutions with different ratio of A^{II} cations. Taking into account the specificity of the investigated samples, the X-ray is the most precise methods, as from one side it measures some volume (mix of phases) of the materials but from the other side, it permits to calculate the parameter of the each one.

Phase diagram of $ZnGeAs_2$–$CdGeAs_2$ was constructed using the obtained results, Fig. 5. The compositions of the samples were taken as were nominal prepared (0.1, 0.2 … 0.9). We strongly believe, that relatively large size of the probe for DTA (1 g.) consists the average nominal concentration of the $ZnGeAs_2$ and $CdGeAs_2$ compounds. The literature data [29] is shown in the diagram with open square symbols. X-ray data is mentioned with closed round symbols. The reporting study is in good agreement with literature data of liquidus and solidus lines, that support our nominal concentrations data. The main cause of the scattered data on phase diagram is mixture of the granules with different compositions.

Table 4
Juxtaposition of the microstructures, DTA, X-ray and EDXRD data.

Sample	Microstructure	DTA (°C)	X-ray X	EDXRD X	Nominal X
1. $ZnGeAs_2$	1 phase	880; 851	0.00	0.00	0.00
2. $Zn_{1-x}Cd_xGeAs_2$	1 phase	868; 800	0.05	0.19	0.10
3. $Zn_{1-x}Cd_xGeAs_2$	2 phases	846; 603; 342	0.13	0.15	0.20
4. $Zn_{1-x}Cd_xGeAs_2$	2 phases	832; 594; 382	0.26	0.23	0.30
5. $Zn_{1-x}Cd_xGeAs_2$	2 phases	809; 670; 422	0.26	0.36	0.40
6. $Zn_{1-x}Cd_xGeAs_2$	2 phases	795; 632; 467	0.39	0.36	0.50
7. $Zn_{1-x}Cd_xGeAs_2$	2 phases	750; 649; 397	0.51	0.62	0.60
8. -$Zn_{1-x}Cd_xGeAs_2$	2 phases	685; 652; 455	0.64	0.67	0.70
9. $Zn_{1-x}Cd_xGeAs_2$	2 phases	662; 650; 381	0.81	0.71	0.80
10. $Zn_{1-x}Cd_xGeAs_2$	1 phase	657; 318	0.94	0.91	0.90
11. $CdGeAs_2$	1 phase	655	1.00	1.00	1.00

4. Conclusions

Phase diagram $ZnGeAs_2$–$CdGeAs_2$ were investigated using X-ray, DTA, microstructures and EXDRF analyses. The solid solutions were observed in full range of concentration above 440 °C. Below this temperature, the dissipation of the solid solution was observed in the range of $Zn_{1-x}Cd_xGeAs_2$ concentration $x = 0.19$–0.92. The investigation of the system is difficult because of liquation and segregation processes occurring during the synthesis. As the results, the compounds have nanosized (20–40 nm) inclusions of compounds with different concentrations. The random distribution of the nano-including into the samples disguises the real solubility in the crystal structures.

Acknowledgements

The reported study was supported by RFBR, research Project No. N 12-03-31203. Scientific work was financed from funds for science in 2011-2014, under the Project No. N202 166840 granted by the National Center for Science of Poland.

References

[1] F. Boukabrine, F. Chiker, H. Khachai, A. Haddou, N. Baki, R. Khenata, B. Abbar, A. Khalfi, Phys. B: Condens. Matter 406 (2011) 169–176.
[2] S.G. Choi, D.E. Aspnes, M. van Schilfgaarde, T.J. Peshek, T.J. Coutts, A.G. Norman, J.M. Olson, D.H. Levi, Optical properties of epitaxial ZnGeAs2 thin film, APS March Meeting, American Physical Society, 2009 (abstract #H21.014).
[3] T.J. Peshek, L. Zhang, R.K. Singh, Z. Tang, M. Vahidi, B. To, T.J. Coutts, T.A. Gessert, N. Newman, M. van Schilfgaarde, Prog. Photovolt. Res. Appl. 21 (2013) 906–917.
[4] T.J. Peshek, Z. Tang, L. Zhang, R.K. Singh, B. To, T.A. Gessert, T.J. Coutts, N. Newman, M. Van Schilfgaarde, ZnGeAs2 thin films properties: a potentially useful semiconductor for photovoltaic applications, in: 34th IEEE Photovoltaic Specialists Conference (PVSC), 2009 pp. 001367–001369.
[5] I.G. Vasilyeva, M.G. Demidova, Talanta 101 (2012) 187–191.
[6] G.A. Verozubova, A.O. Okunev, A.I. Gribenyukov, A.Yu. Trofimiv, E.M. Trukhanov, A.V. Kolesnikov, J. Cryst. Growth 312 (2010) 1122–1126.
[7] V. Kumar, S.K. Tripathy, J. Alloys Comp. 582 (2014) 101–107.
[8] F. Arab, F. Ali Sahraoui, K. Haddadi, L. Louail, Comput. Mater. Sci. 65 (2012) 520–527.
[9] H. Peca-Pedraza, S.A. Lypez-Rivera, J.M. Martin, J.M. Delgado, Ch. Power, Mater. Sci. Eng., B 177 (2012) 1465–1469.
[10] L. Fan, S. Zhu, B. Zhao, B. Chen, Z. He, H. Yang, G. Liu, X. Wang, J. Cryst. Growth 364 (2013) 62–66.
[11] Z. Lv, Y. Cheng, X. Chen, G. Ji, Comput. Mater. Sci. 77 (2013) 114–119.
[12] L. Shen, B. Wang, D. Wu, Z. Jiao, J. Cryst. Growth 383 (2013) 79–83.
[13] M. Romčević, N. Romčević, W. Dobrowolski, L. Kilanski, J. Trajić, D.V. Timotijević, E. Dynowska, I.V. Fedorchenko, S.F. Marenkin, J. Alloys Comp. 548 (2013) 33–37.
[14] N. Uchitomi, H. Endo, H. Oomae, Y. Jinbo, Thin Solid Films 519 (2011) 8207–8211.
[15] V.M. Novotortsev, S.F. Marenkin, T.A. Kupriyanova, I.V. Fedorchenko, L.I. Koroleva, R. Szymczak, L. Kilanski, V. Domuchowski, A.V. Kochura, Russ. J. Inorg. Chem. 54 (2009) 1350–1354.
[16] V.M. Novotortsev, S.F. Marenkin, I.V. Fedorchenko, A.V. Kochura, Russ. J. Inorg. Chem. 55 (2010) 1762–1773.
[17] I.V. Fedorchenko, A.V. Kochura, S.F. Marenkin, A.N. Aronov, et al., IEEE Trans. Magn. 48 (2012) 1581–1584.
[18] J.L. Shay, J.H. Wernick, Ternary Chalcopyrite Semiconductors, Growth, Electronic Properties and Applications, Pergamon, New York, 1975.
[19] L. Kilanski, R. Gorska, W. Dobrowolski, E. Dynowska, M. Wojcik, B.J. Kowalski, J.R. Anderson, C.R. Rotundu, D.K. Maude, S.A. Varnavskiy, I.V. Fedorchenko, S.F. Marenkin, J. Appl. Phys. 108 (2010) 073925.
[20] L. Kilanski, W. Dobrowolski, E. Dynowska, M. Wyjcik, B.J. Kowalski, N. Nedelko, A. Ślawska-Waniewska, D.K. Maude, S.A. Varnavskiy, I.V. Fedorchenko, S.F. Marenkin, Solid State Commun. 151 (2011) 870–873.
[21] H.S. Saini, M. Singh, A.H. Reshak, M.K. Kashyap, J. Alloys Comp. 518 (2012) 74–79.
[22] S.F. Marenkin, V.B. Lazarev, V.Y. Shievchenko, K.A. Sokolovsky, J. Crys. Growth 50 (1980) 761–763.
[23] S.F. Marenkin, V.M. Novotortsev, K.K. Palkina, S.G. Mikhailov, V.T. Kalinnikov, Inorg. Mater. 40 (2004) 93–95.
[24] J.M. Cody, S.H. Risbud, J. Am. Ceram. Soc. 67 (1984) 41–43.
[25] A.I. Gusev, S.V. Rempel, Inorg. Mater. 39 (2003) 43–47.
[26] A.I. Gusev, Doklady Phys. Chem. 392 (2003) 235–239.
[27] Y. Rosenberg, Y. Gelbstein, M.P. Dariel, J. Alloys Comp. 526 (2012) 31–38.
[28] V.M. Novotortsev, I.S. Zakharov, A.V. Kochura, R. Laiho, A. Lashkul, E. Lahderanta, S.F. Marenkin, S.A. Varnavskii, A.V. Molchanov, S.G. Mikhailov, M.S. Shakhov, G.S. Yur'ev, Russ. J. Inorg. Chem. 53 (2008) 1840–1844.
[29] S.H. Risbud, Appl. Phys. A: Mater. Sci. Process. 62 (1996) 519–523.